HHS Public Access

Author manuscript

J Immunol. Author manuscript; available in PMC 2018 January 15.

Published in final edited form as:

J Immunol. 2017 January 15; 198(2): 741–748. doi:10.4049/jimmunol.1601651.

Divergent functions of Toll-like receptor 2 on hematopoietic and non-hematopoietic cells during chronic *Mycobacterium tuberculosis* infection‡

Jill Konowich[*], **Archana Gopalakrishnan**[*], **Jillian Dietzold**[*], **Sheetal Verma**[*], **Kamlesh Bhatt**[*], **Wasiulla Rafi**[†], and **Padmini Salgame**[*]

[*]Department of Medicine, Center for Emerging Pathogens, Rutgers-New Jersey Medical School, Newark, NJ, USA

[†]Ogilvy Commonhealth Worldwide, 440 Interpace Parkway, Parsippany, New Jersey, USA

Abstract

We have reported that Toll-like receptor 2 (TLR2) is crucial for host resistance against chronic *Mycobacterium tuberculosis* (Mtb) infection; however, which cell types are key players in this response remain unknown. This led us to decipher the relative contribution of TLR2 on non-hematopoietic and hematopoietic cells in resistance against chronic Mtb infection in mice infected with Mtb Erdman. Consistent with our previous report, at 8 weeks of infection, TLR2KO→TLR2KO (TLR2KO) bone-marrow chimeric mice exhibited increased bacterial burden, disorganized accumulation of lymphocytes and mononuclear cells, and extensive pulmonary immunopathology compared to WT→WT (WT) chimeric mice. Bacterial burden and pulmonary immunopathology of chimeric mice lacking TLR2 in the hematopoietic compartment [TLR2KO→WT (H-TLR2KO)] was comparable to TLR2KO mice. In contrast, chimeric mice deficient in TLR2 in the non-hematopoietic compartment [WT→TLR2KO (NH-TLR2KO)] exhibited a marked attenuation in granulomatous inflammation compared to WT mice. Although NH-TLR2KO mice did not exhibit improved pulmonary bacterial control, significant reductions in bacterial burden in the draining lymph nodes, spleen, and liver were observed. These findings establish that the TLR2-mediated hematopoietic response promotes stable control of pulmonary bacterial burden and granuloma integrity, while TLR2 signaling on non-hematopoietic cells may partly facilitate granulomatous inflammation and bacterial dissemination.

Introduction

A vast repertoire of mycobacterial ligands are recognized by TLR2, including numerous types of lipoproteins such as LprA, LprG, LpH (19-kDa lipoprotein), PhoS1 (38-kDa lipoprotein), and lipoarabinomannan (LAM) and glycolipids, as well as trehalose mycolate (1–5). Activation of TLR2 signaling by Mtb ligands has been found to modulate multiple APC functions, which are essential to eliciting and controlling an immune response to Mtb

‡This work was supported by the NIH AI0848221 to PS.

Corresponding Author: Padmini Salgame, Department of Medicine, Center for Emerging Pathogens, MSB A901, Rutgers-New Jersey Medical School, Newark, NJ 07101, USA, Tel # 973 972 8647, Fax # 973 972 0713, salgampa@njms.rutgers.edu.

(6, 7). Purified Mtb lipoproteins, including LpqH, LprG and LprA, have been identified to induce both stimulatory and inhibitory effects on host APCs via TLR2 (2–4). TLR2-directed Mtb ligands stimulate expression of multiple cytokines including TNF, IL-12, IL-10 and secretory protease inhibitor (8) by macrophages and dendritic cells (DCs) (3, 4, 9, 10) and enhancement of DC maturation (3, 11).

TLR2 activation also generates direct antimicrobial activity by augmenting expression of the vitamin D receptor and vitamin D hydroxylase resulting in up-regulation of antimicrobial peptides (9) and reciprocally the absence of TLR2 on Mtb-infected macrophages results in reduced antibacterial activity (12). TLR2 signaling by Mtb has also been associated with inhibition of macrophage responses. *In vitro* studies have shown that engagement of TLR2 with Mtb ligands blocks macrophage responsiveness to IFNγ (13, 14) and prolonged exposure to Mtb lipoproteins inhibits IFNγ-induced expression of class II transactivator (CIITA), class II MHC (MHC-II), and MHC-II-restricted antigen presentation by macrophages (3–5, 14, 15). Furthermore, Mtb induction of the immunosuppressive cytokine IL-10 from DCs and macrophages is TLR2-dependent (16).

Except for one group (12), we and others found that TLR2-deficient (TLR2KO) mice are resistant to acute infection when infected with a low dose of Mtb (17–20). However, by extending the studies into the chronic phase, we determined that TLR2KO mice are unable to maintain stable bacterial burden, resulting in exaggerated immunopathology characterized by pneumonitis and enhanced cellular infiltration (21). We also found that TLR2 plays a key role in T regulatory cell (Treg) recruitment to the lungs and contributes significantly to maintaining the integrity of the tubercle granuloma in chronic infection (21). TLR2 polymorphisms, particularly within the TIR domain, have been associated with increased susceptibility to pulmonary tuberculosis (TB) and an increased risk of extrapulmonary TB (22–27). Analysis of a polymorphic guanine-thymine (GT) repeat located upstream of the TLR2 translational start site correlated shorter GT repeats with development of TB and lower TLR2 expression (28). Although the mechanism behind how these polymorphisms affect the immune response to Mtb is unclear, nonetheless, these correlations suggest an important role for TLR2 in host defense against Mtb.

Recent studies have illustrated a role for pulmonary epithelium in regulating the immune response to Mtb. Alveolar epithelial cells can phagocytose mycobacteria using syndecans (29) and also produce pro-inflammatory cytokines and chemokines in response to Mtb infection, including TNF, IFNγ, CXCL8, CCL5, IL-1β, IL-6, IL-18, and MCP-1, which play central roles in cellular recruitment (30). Mycobacteria can also promote the secretion of IL-10 and IL-22, anti-inflammatory cytokines, from alveolar epithelial cells by inhibiting NFκB signaling in these cells (31). Furthermore, IFNγR on lung epithelial and endothelial cells is essential for controlling IL-17 expression and associated neutrophilic inflammation (32). Consistent with this finding, chimeric mice lacking IFNγR in the non-hematopoietic compartment are highly susceptible to Mtb infection (32). In *Mycobacterium marinum*-infected zebrafish, epithelial cells have been implicated in regulating nascent granuloma maturation and bacterial growth; within epithelial cells, ESAT-6 was shown to induce MMP9 secretion, thereby enhancing cellular recruitment to sites of infection (33). Given that TLR2 is highly expressed on airway epithelial cells (34) and Mtb mediates cytokine

responses from these cells in a TLR2-dependent manner (35, 36), we consequently focused this current study on dissecting the functions of TLR2 in the hematopoietic and non-hematopoietic compartments in controlling chronic Mtb infection. Bone marrow chimeric mice lacking TLR2 either in the hematopoietic compartment, non-hematopoietic compartment, or both were generated to investigate each compartment's respective contribution to host resistance during the chronic phase of Mtb infection.

Materials and Methods

Mice

C57Bl/6 and B6-Ly5.2 congenic mice were purchased from Charles River NCI (Fredrick, MD). TLR2KO mice were developed by S. Akira and colleagues (37) and provided to us by Alan Sher (NIH). TLR2KO mice were bred and maintained under pathogen-free conditions at the transgenic animal facility at the Rutgers-NJMS. Female mice were studied at 6–10 weeks of age. Mtb-infected mice were housed in the biosafety level 3 (BSL3) facility at the Public Health Research Institute at Rutgers-NJMS. Animal protocols used in this study were approved by the Rutgers IACUC.

Chimera generation

Radiation bone marrow chimeric mice which were WT or lacking TLR2 either in the hematopoietic compartment (H-TLR2KO), non-hematopoietic (NH-TLR2KO) compartment, or both (TLR2KO) were generated. Recipient mice were fasted overnight before irradiation. Recipient mice were loaded into an irradiation chamber and received a split dose of 600 Rads (6 Gray) (ca. 2 minutes per chamber). Irradiation rounds were spaced 2 hours apart. After the second dose, fasting recipient mice were rested in their colony for 6 hours before reconstitution with donor bone marrow. Donor B6-Ly5.2 congenic ($CD45.1^+$) and TLR2KO ($CD45.2^+$) mice were euthanized with CO_2 asphyxiation, and femurs and tibias were removed aseptically. Bone marrow was flushed with cold DMEM (Invitrogen) supplemented with 10% heat-inactivated fetal calf serum (FCS) (Invitrogen) and 2mM L-glutamine (Invitrogen) and pelleted. Cells were washed twice with sterile PBS (Invitrogen) with 1% fetal calf serum. Mature T cells were depleted from the suspension by adding microbeads coated with anti-Thy1.2 antibody (Miltenyi Biotec), which was followed by magnetic-activated cell sorting (according to manufacturer's protocol). Viable cells were counted by trypan blue exclusion assay. At 6 hours after the second dose of radiation, recipient mice were reconstituted with 5×10^6 donor cells by intravenous retro-orbital injection. Food was returned to the mice and they were given an oral suspension of sulfamethoxazole (150mg/mL) and trimethoprim (30mg/mL) in their drinking water for 3 weeks.

Chimeras were infected with Mtb after 6 weeks of transplantation. Before infection, reconstitution of all chimeric mice was confirmed by tail bleeds. Successful chimerism was confirmed by assessing the population of $CD45.1^+$ and $CD45.2^+$ cells in lungs, blood, spleen, and lymph nodes. We confirmed at least 85% chimerism by assessing the percentage of $CD45.1^+$ and $CD45.2^+$ in overall leukocytes and specifically T cells, B cells, macrophages, monocytes, and dendritic cells through surface staining with fluorochrome-

conjugated monoclonal antibodies. These levels did not vary over time after Mtb-infection. At each time point, percentage of $CD45.1^+$ and $CD45.2^+$ cells in leukocyte populations was assessed in lungs and spleen.

Mouse aerosol infections

The virulent Erdman strain (Trudeau Institute, Saranac Lake, NY) of Mtb was used for all mouse infections. Bacterial stocks were generated by initial passage through C57Bl/6 mice. Bacterial colonies obtained from lung homogenates were grown in 7H9 media until mid-log phase, and the culture was stored in 1 mL aliquots at −80°C. The stock titer was determined by plating 10-fold serial dilutions on Middlebrook 7H11 selective medium (Difco BD, Franklin Lakes, NJ). Female mice (age 6–10 weeks) were infected using a closed-air nose only aerosolization system (In-TOX Products, Albuquerque, NM) for most experiments or Glas-Col Full Body Inhalation Exposure System. For experiments using In-TOX products, mice were exposed for 20 minutes to nebulized bacteria at a density optimized to deliver a standard low dose of around 100 CFU (unless otherwise indicated). For experiments using the Glas-Col machinery, mice were exposed for 30 minutes to nebulized bacteria at a density optimized to deliver either a standard low dose of ~50 CFU or a high dose of ~500 CFU. For all infections, the actual infection dose was determined by plating total lung homogenates from a minimum of 5 mice on Middlebrook 7H11 plates at 24 hours after aerosol exposure.

Determination of bacterial burden

At each time interval studied, infected animals were sacrificed by cervical dislocation. Lungs, spleens, lymph nodes, and livers were harvested at indicated time points post infection. Harvested tissues were homogenized in phosphate-buffered saline (PBS) containing 0.05% Tween-80. Total colony forming units (CFU) per organ was determined by plating 10-fold serial dilutions on Middlebrook 7H11 plates. CFU were counted after 21 days of incubation at 37°C. The right superior lobe of the lung was used for determining bacterial burden. The right lower lobe was reserved for histological studies. The right middle lobe was reserved for protein determination. The postcaval lobe was reserved for tissue gene expression. The remaining lung tissue was used for isolation of lung leukocytes. Spleen and lymph nodes were used for bacterial burden and isolation of leukocytes. Liver was used for determination of bacterial burden.

Flow cytometry

In order to obtain single-cell suspensions, lungs were perfused with 10ml of sterile PBS and then harvested. Lung tissue was cut into small pieces and digested with 2mg/mL collagenase D (Roche) for 30 minutes at 37°C. The digestion was stopped by adding 10mM EDTA. The digested tissue was transferred to a 40μm pore nylon cell strainer (BD Falcon) and mashed through using a syringe plunger, and the suspensions were centrifuged for 10 min at 1200 rpm. The collagenase solution was discarded, and the cell pellet was resuspended in ammonium-chloride-potassium (ACK) lysing buffer (Quality Biological, Inc) to remove red blood cells (RBCs). Viable cell number per tissue was determined by trypan blue dye exclusion.

For surface staining, approximately 1 million cells were washed and resuspended in FACS buffer (PBS + 2% fetal calf serum (FCS) and 0.09% sodium azide) containing a cocktail with the appropriate concentrations of specific fluorochrome-conjugated monoclonal antibodies. The following monoclonal antibodies were used in the studies: CD45.1 (clone A20; FITC), CD45.2 (clone 104; V450), CD4 (clone RM4–5; V500), CD8 (clone 53–6.7; APC), Foxp3 (clone FJK-16s; PE), GR1 (RB6-8C5; PeCy7), Ly6C (AL-21; PerCPCy5), CD11c (clone HL3; AF700) and CD11b (clone M1/70; PE). Antibodies to Foxp3, CD45.1, and CD45.2 were purchased from eBioscience. The remaining antibodies were purchased from BD Biosciences. Following surface staining, samples were fixed in 4% paraformaldehyde for 30 minutes and then acquired on a LSRII flow cytometer (BD Biosciences). For enumerating innate cell subsets, cells were first gated on $CD45.1^+$ cells and then the $CD4^-CD8^-$ population was gated on. A side scatter plot for CD11b was used to gate on $CD11b^{hi}$ SSC^{hi} cells and from this population $Gr\text{-}1^+$ cells were gated on. The $CD11b^{hi}SSC^{hi}Gr\text{-}1^+$ cells were defined as the neutrophil population. With the remaining cells that were $CD11b^+SSC^{lo}$, CD11b and CD11c gates were set-up to determine the $CD11b^+CD11c^-$ and $CD11b^-CD11c^+$ populations. From the $CD11b^+CD11c^-$ population, cells that were $Ly6C^+$ were gated on. The $CD11b^+SSC^{lo}Ly6C^+$ cells were defined as the inflammatory monocyte population. The number of cells for the indicated population in the lungs, as noted on the graph, was determined by multiplying the percentages of gated cells by total lung cell number. For enumerating $CD4^+Foxp3^+$Tregs, cells were first surface stained followed by fixation, permeabilization, and intracellular staining with anti-Foxp3 antibodies according to the manufacturer's protocol (eBioscience). Analysis was performed using FlowJo software (Tree Star, Inc.). Gating was based on isotype and fluorescence minus one (FMO) controls.

Histology

Mtb-infected mice were sacrificed at the indicated time intervals, and the lungs were perfused with 10 ml of sterile PBS. Lung tissue was excised and fixed in 4% paraformaldehyde for 4 days, followed by paraffin embedding. For histopathological analysis, 5 to 7μM sections were cut and stained using a standard H&E protocol. For quantitation of percent granulomatous inflammation in the lung section, photomicrographs of H&E stained lung sections were captured using a 5x objective lens. A 546-point grid overlay was superimposed onto each image using Image-Pro Discovery Software, and the numbers of points hitting areas of granulomatous infiltration were counted. The percentage of affected lung tissue was calculated as number of involved points/total points per section × 100.

RNA isolation and real-time PCR

Lung lobes were homogenized in 1ml of TRIzol reagent in lysing matrix D tubes (MP Biomedicals) using a FastPrep homogenizer (MP Biomedicals). Samples were immediately stored at −80°C following lysis in TRIzol. Total RNA was extracted via the manufacturer's TRIzol/chloroform method and purified using RNeasy columns (Qiagen). Total RNA was reverse transcribed into cDNA using Superscript II RT (Invitrogen) and Real-time PCR was performed. Total RNA from uninfected lungs was used as calibrator. Beta-actin was used as

the house keeping gene to normalize gene expression. Baseline gene expression from uninfected WT and KO was equivalent.

Results

Long-term control of Mtb infection is mediated by TLR2 on hematopoietic cells

To distinguish TLR2's role on hematopoietic and non-hematopoietic cells in mediating host resistance against chronic Mtb infection, four groups of radiation bone marrow chimeric mice i) WT→WT (WT); ii) TLR2KO→TLR2KO (TLR2KO); iii) TLR2KO→WT (H-TLR2KO); iv) WT→TLR2KO (NH-TLR2KO) were aerosol-infected with a low inoculum of Mtb, approximately 100 CFU, 6 weeks following irradiation and reconstitution. WT and TLR2KO bone marrow chimeric mice were generated to ensure that the irradiation and reconstitution did not affect the previously observed responses to Mtb infection. Pulmonary bacterial burden was monitored over 14 weeks of infection. At 8 weeks following infection, TLR2KO chimeric mice had a significantly higher pulmonary bacterial load compared to WT chimeric mice, confirming our previous findings (21). Akin to TLR2KO mice, H-TLR2KO chimeric mice had bacterial burden significantly higher than WT mice (Fig. 1A). Similar differences in CFU were also seen at 14 weeks of infection (Fig. 1B). These results provide evidence that TLR2 signaling on hematopoietic cells mediates the stable maintenance of bacterial burden during chronic Mtb infection.

Consistent with the higher bacterial load, expression of *Tnf* and *Ifnγ* was increased in H-TLR2KO and in TLR2KO mice compared to WT mice at week 8 of infection. No differences in *Tnf* and *Ifnγ* expression was found between NH-TLR2KO and WT mice (Fig. 1C).

Dissemination of Mtb to extrapulmonary sites is decreased in the absence of TLR2 on non-hematopoietic cells

We next investigated whether absence of TLR2 on either hematopoietic or non-hematopoietic cells affects dissemination to extrapulmonary organs. Spleen, liver, and mediastinal lymph nodes (MLN), were harvested at weeks 8 and 14 (Fig. 2) to evaluate the dissemination of Mtb from the lungs. We observed no difference in CFU between WT, TLR2KO and H-TLR2KO chimeric mice in spleen, liver or MLN during the chronic phase of infection (weeks 8 and 14) (Fig. 2). Therefore, dissemination to extrapulmonary organs is independent of TLR2 on hematopoietic cells. Interestingly, there was significantly decreased dissemination of Mtb to the spleen, liver, and MLN in the NH-TLR2KO mice as compared to the three groups. These data indicate that TLR2 signaling on non-hematopoietic cells facilitates the dissemination of Mtb to extra-pulmonary organs during chronic infection.

Differential granulomatous response in H-TLR2KO and NH-TLR2KO chimeric mice

The development of pulmonary pathology in H&E stained sections of infected chimeric mice was next characterized. As shown in Figure 3A, at 8 weeks following infection, WT mice display a typical controlled response to Mtb infection with formation of compact granulomas (G) and conspicuous lymphocytic aggregates (L). Consistent with our published work (21) and that of others (17, 38), chronically infected TLR2KO mice did not show

compact granulomas and instead exhibited increased inflammation (I) (Fig. 3C) in comparison to WT mice (Fig. 3A). Similarly, H-TLR2KO mice exhibited extensive inflammation (I) and lacked compact granulomas (Fig. 3D). In both TLR2KO (Fig. 3C) and H-TLR2KO (Fig. 3D) chimeric mice, lymphocytic aggregates were smaller and less apparent, and the lung tissue exhibited a marked increase in cellularity, especially in the perivascular and bronchial areas. Inflammation induced pathology extended into most of the lung parenchyma in both the H-TLR2KO and TLR2KO chimeric mice and can be correlated with the significant increase in bacterial burden observed in these mice. The overall histopathological response of NH-TLR2KO chimeric mice, on the other hand, was similar to that of WT mice, as both exhibit immunopathology confined to granulomas (Fig. 3B). These histopathological differences were also observed in 14-week infected lungs as well (data not shown).

Consistent with the histopathological response, H-TLR2KO and TLR2KO chimeric mice had increased recruitment of $CD11b^{hI}Gr\text{-}1^{+}$ neutrophils and $CD11b^{+}Ly6C^{+}$ inflammatory monocytes, albeit not statistically significant. On the other hand, NH-TLR2KO lungs exhibited an overall reduced recruitment of inflammatory innate immune cells, including $CD11b^{+}CD11c^{-}$ recruited macrophages, $CD11b^{-}CD11c^{+}$ alveolar macrophages, $CD11b^{hI}Gr\text{-}1^{+}$ neutrophils and $CD11b^{+}Ly6C^{+}$ inflammatory monocytes (Fig. 3E). These trends parallel the differences in inflammation observed in the lungs and reinforce that TLR2 signaling on non-hematopoietic cells may contribute to increased cellular recruitment and pulmonary inflammation.

We further examined the mosaic images of H&E stained lungs of WT and NH-TLR2KO mice and it revealed unexpected findings. NH-TLR2KO mice displayed more compact granulomas with less pulmonary pneumonitis (Fig. 4A and 4B). To confirm these observations, we examined pulmonary inflammation outside of granulomatous tissue in WT and NH-TLR2KO mice (Fig. 4A and 4B). Areas outside the granulomatous inflammation in the lung parenchyma were chosen in WT and NH-TLR2KO sections from acquired mosaic images. The sections analyzed are boxed in Figure 4, panels A and B. Stark differences in parenchymal inflammation are noticeable upon closer examination of alveolar spaces (Fig. 4C and Fig. 4D). The alveoli in the NH-TLR2KOs display single layers of type I (long arrow) and type II (arrowhead) pneumocytes and endothelial capillaries with minimal inflammation, indicative of healthier lung tissue (Fig. 4D). A comparable image taken from WT lung parenchyma displays increased cellular infiltration between these cell layers. Distinct alveolar spaces are more apparent in NH-TLR2KO as compared with WT lung tissue (Fig. 4C and Fig. 4D). WT alveolar spaces are visible but difficult to distinguish. Within this section of WT lung tissue, there are no pulmonary alveolar spaces lined by a single layer of cells.

To quantify what we have qualitatively detailed, the percent lung area involved in granulomatous inflammation was calculated from lung photomicrographs from WT, NH-TLR2KO, H-TLR2KO, and TLR2KO mice. Granulomatous inflammation in both H-TLR2KO and TLR2KO lung tissue was significantly higher as compared to WT lung tissue at both weeks 8 and 14 (Fig. 4E). Percent inflammation in H-TLR2KO mice ranged from 60–80% at week 8 and 55–90% at week 14 (Fig. 4E). TLR2KO mice demonstrated similar

results. In contrast, the NH-TLR2KO mice displayed significantly reduced lung area involved in granulomatous inflammation as compared to the other groups (Fig. 4E). The NH-TLR2KO mice displayed significantly lower inflammation at week 8. The range in inflammation for the NH-TLR2KO mice exhibited no overlap with WT chimeric mice. Similarly, at week 14, NH-TLR2KO mice had significantly lower inflammation as compared with WT mice. Reduced granulomatous areas in the NH-TLR2KO chimeric mice correlate with a significantly lower percentage of lung area involved in TB infection as opposed to WT mice (Fig. 4A–D). Together, these findings indicate that intact TLR2 signaling on WT non-hematopoietic cells may contribute towards TB-induced pathology in the lung parenchyma.

Recruitment of Tregs to the lungs is regulated by the hematopoietic compartment

Because the H-TLR2KO chimeric mice displayed similar pathology to TLR2KO chimeric mice, we next determined whether the Treg phenotype of the H-TLR2KO chimeric mice would be similar to the TLR2KO chimeric mice. Flow cytometric analysis of lung cells of 8 week-infected chimeric mice showed that the percentage of $CD4^+$ T cells remained similar between the four groups of chimeric mice (Fig. 5A). Consistent with our previous finding, TLR2KO chimeric mice accumulated significantly less $CD4^+Foxp3^+$ Tregs in their lungs compared to WT mice. Akin to the TLR2KO, H-TLR2KO chimeric mice also exhibited a marked decrease in $CD4^+Foxp3^+$ Tregs as compared with WT and NH-TLR2KO chimeric mice (Fig 5.B). The percentage of $CD4^+Foxp3^+$ Tregs in NH-TLR2KO chimeric mice was similar to WT chimeric mice. These data strengthen the immunoregulatory role of TLR2 and demonstrates that Treg recruitment is dependent on TLR2 on the hematopoietic cells.

Discussion

In this study we analyzed the compartment-specific function of TLR2 in host resistance against Mtb infection. We found that TLR2 on hematopoietic cells was necessary for stable control of bacterial growth and in maintaining granuloma integrity during chronic infection. TLR2 on hematopoietic cells also regulated Treg accumulation in the lung. Furthermore, the results suggest that TLR2 on non-hematopoietic cells may contribute to the pulmonary inflammation present during the chronic phase of infection which directly or indirectly may facilitate bacterial dissemination. Together, the findings from the study point to paradoxical roles for TLR2 on hematopoietic and non-hematopoietic cells.

There are abundant examples from *in vitro* work demonstrating that TLR2 engagement activates anti-bacterial responses in macrophages. In a series of studies, Modlin and colleagues have delineated the role of the vitamin D3-dependent cathelicidin pathway in killing of intracellular Mtb (39). Their studies implicate that TLR2-mediated activation of human macrophages is one of the principal pathway that activates the vitamin D3-dependent cathelicidin pathway (39). TLR2 signaling also engages the vitamin D/cathelicidin pathway to trigger anti-bacterial autophagy (40). Antimicrobial responses from TLR2 are also triggered via its interaction with NADPH oxidase 2 (41). Besides direct activation of microbicidal pathways, the operant mechanism of Mtb growth restriction by TLR2 could also be indirect. PAMPs can mediate recruitment of microbicidal macrophages, but PAMPS

are masked by cell-surface-associated phthiocerol dimycoceroserate (PDIM) lipids. These exposed PDIMs on intact bacteria, instead, recruit $CCR2^+$ permissive macrophages (42). Mtb can release extracellular mycobacterial vesicles (MV) that are enriched for TLR2 ligands (43, 44) and the TLR2 ligand, 19kda lipoprotein, can also be secreted via the SecA1 pathway (45). This indicates that within the mature granuloma, TLR2 agonists can be secreted and potentially engage TLR2 on hematopoietic cells to recruit microbicidal macrophages and control chronic infection. Consequently, in the absence of TLR2 on hematopoietic cells, signaling from lipids, such as PDIM, may dominate leading to the recruitment of permissive macrophages and unrestricted Mtb growth. Exploring whether the underlying mechanism for stable control of Mtb in chronic infection is the activation of direct or indirect pathways by TLR2 on hematopoietic cells may provide means to enhance Mtb killing in the granuloma.

The mature granuloma is a dynamic structure and cells traffic in and out of this microenvironment (46). The finding that NH-TLR2KO mice exhibited decreased inflammation and reduced hematogenous spread suggests that TLR2 signaling on non-hematopoietic cells may serve as one pathway of mediating the continuous recruitment and egress of immune cells to and from the granuloma. New macrophages that are recruited to the granuloma may provide new niches for Mtb and the exit of infected macrophages may promote the formation of new granulomas and hematogenous spread (47). Macrophage recruitment to the granulomas could be mediated through MMP9 secretion from cells of the non-hematopoietic compartment since Mtb-secreted protein 6-kD early secreted antigenic target (ESAT-6) can induce MMP9 secretion from epithelial cells (33). Mycobacterial infection upregulates TLR2 expression on airway epithelial cells and blocking of TLR2 inhibits secretion of CXCL8 and IL-6 and consequent neutrophil recruitment (35) suggests that TLR2 activation on airway epithelial cells could also enhance inflammation in the lung via recruitment of neutrophils. Overall, our finding that TLR2 signaling on non-hematopoietic cells is a significant regulator of the granuloma microenvironment provides opportunities for cell-specific blocking of TLR2 to curtail pulmonary inflammation.

Following a high dose of Mtb infection, CXCL5-deficient mice demonstrate reduced neutrophil recruitment to the lungs and do not develop subsequent destructive pulmonary inflammation. The CXCL5-deficient mice, in fact, exhibit heightened resistance to Mtb infection (48). This study also reported that CXCL5 induction from epithelial cells was TLR2-mediated (48). Our finding that the granulomatous inflammation is significantly reduced in the NH-TLR2KO mice is consistent with the above study. However, despite reduced inflammation, we did not observe increased resistance even at 14 weeks following infection in the NH-TLR2KO mice. In our study, mice were infected with a low dose of Mtb Erdman which does not elicit detrimental excessive inflammation in the WT setting, and so the removal of TLR2 probably did not impact host resistance in a significant way. Nonetheless, the insight provided by this study highlights the potential pathological role that TLR2 could play in the NH compartment when the host is infected with Mtb that induces excessive inflammation. In this context, development of disseminated TB has been reported to be dually influenced by Mtb strain and TLR2 polymorphism (49). Clearly, ascertaining the role of TLR2 in the non-hematopoietic compartment in response to infection with clinical strains will be significant.

A recent study identified a gene (*rv0431*) that regulates mycobacterial vesicle formation and named it the “vesiculogenesis and immune response regulator” (*virR*) (50). VirR-deficient Mtb were hyper-inflammatory and their vesicles were enriched for TLR2 ligands in comparison to vesicles isolated from WT Mtb. Mouse infections revealed that the growth of the VirR-deficient Mtb was attenuated in WT but not in TLR2KO mice (50) indicating that host resistance can be improved by increasing the quantity of TLR2 ligands. This suggests that understanding the regulation of TLR2 ligand secretion is a potentially rich area for further investigations.

Overall, the current study demonstrates a definitive role for TLR2 in host defense and provides evidence that TLR2 on hematopoietic cells contributes to the protective functions in a non-redundant manner. Additional studies with clinical strains of Mtb are required to fully understand the pathology-inducing role of TLR2 on non-hematopoietic cells.

References

1. Drage MG, Pecora ND, Hise AG, Febbraio M, Silverstein RL, Golenbock DT, Boom WH, Harding CV. TLR2 and its co-receptors determine responses of macrophages and dendritic cells to lipoproteins of Mycobacterium tuberculosis. Cell Immunol. 2009; 258:29–37. [PubMed: 19362712]
2. Sutcliffe IC, Harrington DJ. Lipoproteins of Mycobacterium tuberculosis: an abundant and functionally diverse class of cell envelope components. FEMS Microbiol Rev. 2004; 28:645–659. [PubMed: 15539077]
3. Pecora ND, Gehring AJ, Canaday DH, Boom WH, Harding CV. Mycobacterium tuberculosis LprA is a lipoprotein agonist of TLR2 that regulates innate immunity and APC function. J Immunol. 2006; 177:422–429. [PubMed: 16785538]
4. Gehring AJ, Dobos KM, Belisle JT, Harding CV, Boom WH. Mycobacterium tuberculosis LprG (Rv1411c): a novel TLR-2 ligand that inhibits human macrophage class II MHC antigen processing. J Immunol. 2004; 173:2660–2668. [PubMed: 15294983]
5. Noss EH, Pai RK, Sellati TJ, Radolf JD, Belisle J, Golenbock DT, Boom WH, Harding CV. Toll-like receptor 2-dependent inhibition of macrophage class II MHC expression and antigen processing by 19-kDa lipoprotein of Mycobacterium tuberculosis. J Immunol. 2001; 167:910–918. [PubMed: 11441098]
6. Harding CV, Boom WH. Regulation of antigen presentation by Mycobacterium tuberculosis: a role for Toll-like receptors. Nat Rev Microbiol. 2010; 8:296–307. [PubMed: 20234378]
7. Kawai T, Akira S. TLR signaling. Cell Death Differ. 2006; 13:816–825. [PubMed: 16410796]
8. Ding A, Yu H, Yang J, Shi S, Ehrt S. Induction of macrophage-derived SLPI by Mycobacterium tuberculosis depends on TLR2 but not MyD88. Immunology. 2005; 116:381–389. [PubMed: 16236128]
9. Brightbill HD, Libraty DH, Krutzik SR, Yang RB, Belisle JT, Bleharski JR, Maitland M, Norgard MV, Plevy SE, Smale ST, Brennan PJ, Bloom BR, Godowski PJ, Modlin RL. Host defense mechanisms triggered by microbial lipoproteins through toll-like receptors. Science. 1999; 285:732–736. [PubMed: 10426995]
10. Thomas-Uszynski S, Kiertscher SM, Ochoa MT, Bouis DA, Norgard MV, Miyake K, Godowski PJ, Roth MD, Modlin RL. Activation of Toll-like receptor 2 on human dendritic cells triggers induction of IL-12 but not IL-10. J Immunol. 2000; 165:3804. [PubMed: 11034386]
11. Hertz CJ, Kiertscher SM, Godowski PJ, Bouis DA, Norgard MV, Roth MD, Modlin RL. Microbial lipopeptides stimulate dendritic cell maturation via Toll-like receptor 2. J Immunol. 2001; 166:2444–2450. [PubMed: 11160304]
12. Tjarnlund A, Guirado E, Julian E, Cardona PJ, Fernandez C. Determinant role for Toll-like receptor signalling in acute mycobacterial infection in the respiratory tract. Microbes Infect. 2006; 8:1790–1800. [PubMed: 16815067]

13. Fortune SM, Solache A, Jaeger A, Hill PJ, Belisle JT, Bloom BR, Rubin EJ, Ernst JD. Mycobacterium tuberculosis inhibits macrophage responses to IFN-gamma through myeloid differentiation factor 88-dependent and -independent mechanisms. J Immunol. 2004; 172:6272–6280. [PubMed: 15128816]
14. Banaiee N, Kincaid EZ, Buchwald U, Jacobs WR Jr, Ernst JD. Potent inhibition of macrophage responses to IFN-gamma by live virulent Mycobacterium tuberculosis is independent of mature mycobacterial lipoproteins but dependent on TLR2. J Immunol. 2006; 176:3019–3027. [PubMed: 16493060]
15. Pennini ME, Pai RK, Schultz DC, Boom WH, Harding CV. Mycobacterium tuberculosis 19-kDa lipoprotein inhibits IFN-gamma-induced chromatin remodeling of MHC2TA by TLR2 and MAPK signaling. J Immunol. 2006; 176:4323–4330. [PubMed: 16547269]
16. Jang S, Uematsu S, Akira S, Salgame P. IL-6 and IL-10 induction from dendritic cells in response to Mycobacterium tuberculosis is predominantly dependent on TLR2-mediated recognition. J Immunol. 2004; 173:3392–3397. [PubMed: 15322203]
17. Drennan MB, Nicolle D, Quesniaux VJ, jacobs M, Allie N, Mpagi J, Fremond C, Wagnet H, Kirschning CJ, Ryffel B. Toll-Like receptor 2-deficient mice succumb to Mycobacterium tuberculosis infection. Am J pathol. 2004; 164:49–57. [PubMed: 14695318]
18. Reiling N, Holscher C, Fehrenbach A, Kroger S, Kirschning CJ, Goyert S, Ehlers S. Cutting edge: Toll-like receptor (TLR)2- and TLR4-mediated pathogen recognition in resistance to airborne infection with Mycobacterium tuberculosis. J Immunol. 2002; 169:3480–3484. [PubMed: 12244136]
19. Sugawara I, Yamada H, Li C, Mizuno S, Takeuchi O, Akira S. Mycobacterial infection in TLR2 and TLR6 knockout mice. Microbiol Immuno. 2003; 47:327–336.
20. McBride A, Bhatt K, Salgame P. Development of a secondary immune response to Mycobacterium tuberculosis is independent of Toll-like receptor 2. Infect Immun. 2011; 79:1118–1123. [PubMed: 21173309]
21. McBride A, Konowich J, Salgame P. Host Defense and Recruitment of Foxp3(+) T Regulatory Cells to the Lungs in Chronic Mycobacterium tuberculosis Infection Requires Toll-like Receptor 2. PLoS Pathog. 2013; 9:e1003397. [PubMed: 23785280]
22. Dalgic N, Tekin D, Kayaalti Z, Soylemezoglu T, Cakir E, Kilic B, Kutlubay B, Sancar M, Odabasi M. Arg753Gln polymorphism of the human Toll-like receptor 2 gene from infection to disease in pediatric tuberculosis. Hum Immunol. 2011; 72:440–445. [PubMed: 21320563]
23. Motsinger-Reif AA, Antas PR, Oki NO, Levy S, Holland SM, Sterling TR. Polymorphisms in IL-1beta, vitamin D receptor Fok1, and Toll-like receptor 2 are associated with extrapulmonary tuberculosis. BMC Med Genet. 2010; 11:37. [PubMed: 20196868]
24. Shah JA, Vary JC, Chau TT, Bang ND, Yen NT, Farrar JJ, Dunstan SJ, Hawn TR. Human TOLLIP regulates TLR2 and TLR4 signaling and its polymorphisms are associated with susceptibility to tuberculosis. J Immunol. 2012; 189:1737–1746. [PubMed: 22778396]
25. Ogus AC, Yoldas B, Ozdemir T, Uguz A, Olcen S, Keser I, Coskun M, Cilli A, Yegin O. The Arg753GLn polymorphism of the human toll-like receptor 2 gene in tuberculosis disease. Eur Respir J. 2004; 23:219–223. [PubMed: 14979495]
26. Ben-Ali M, Barbouche MR, Bousnina S, Chabbou A, Dellagi K. Toll-like receptor 2 Arg677Trp polymorphism is associated with susceptibility to tuberculosis in Tunisian patients. Clin Diagn Lab Immunol. 2004; 11:625–626. [PubMed: 15138193]
27. Velez DR, Wejse C, Stryjewski ME, Abbate E, Hulme WF, Myers JL, Estevan R, Patillo SG, Olesen R, Tacconelli A, Sirugo G, Gilbert JR, Hamilton CD, Scott WK. Variants in toll-like receptors 2 and 9 influence susceptibility to pulmonary tuberculosis in Caucasians, African-Americans, and West Africans. Hum Genet. 2010; 127:65–73. [PubMed: 19771452]
28. Yim JJ, Lee HW, Lee HS, Kim YW, Han SK, Shim YS, Holland SM. The association between microsatellite polymorphisms in intron II of the human Toll-like receptor 2 gene and tuberculosis among Koreans. Genes Immun. 2006; 7:150–155. [PubMed: 16437124]
29. Zimmermann N, Saiga H, Houthuys E, Moura-Alves P, Koehler A, Bandermann S, Dorhoi A, Kaufmann SH. Syndecans promote mycobacterial internalization by lung epithelial cells. Cell Microbiol. 2016

30. Li Y, Wang Y, Liu X. The role of airway epithelial cells in response to mycobacteria infection. Clinical & developmental immunology. 2012; 2012:791392. [PubMed: 22570668]

31. Lutay N, Hakansson G, Alaridah N, Hallgren O, Westergren-Thorsson G, Godaly G. Mycobacteria bypass mucosal NF-kB signalling to induce an epithelial anti-inflammatory IL-22 and IL-10 response. PLoS One. 2014; 9:e86466. [PubMed: 24489729]

32. Desvignes L, Ernst JD. Interferon-gamma-responsive nonhematopoietic cells regulate the immune response to Mycobacterium tuberculosis. Immunity. 2009; 31:974–985. [PubMed: 20064452]

33. Volkman HE, Pozos TC, Zheng J, Davis JM, Rawls JF, Ramakrishnan L. Tuberculous granuloma induction via interaction of a bacterial secreted protein with host epithelium. Science. 2010; 327:466–469. [PubMed: 20007864]

34. Armstrong L, Medford AR, Uppington KM, Robertson J, Witherden IR, Tetley TD, Millar AB. Expression of functional toll-like receptor-2 and -4 on alveolar epithelial cells. Am J Respir Cell Mol Biol. 2004; 31:241–245. [PubMed: 15044215]

35. Andersson M, Lutay N, Hallgren O, Westergren-Thorsson G, Svensson M, Godaly G. Mycobacterium bovis bacilli Calmette-Guerin regulates leukocyte recruitment by modulating alveolar inflammatory responses. Innate Immun. 2012; 18:531–540. [PubMed: 22058091]

36. Sequeira PC, Senaratne RH, Riley LW. Inhibition of toll-like receptor 2 (TLR-2)-mediated response in human alveolar epithelial cells by mycolic acids and Mycobacterium tuberculosis mce1 operon mutant. Pathog Dis. 2014; 70:132–140. [PubMed: 24190334]

37. Takeuchi O, Hoshino K, Kawai T, Sanjo H, Takada H, Ogawa T, Takeda K, Akira S. Differential roles of TLR2 and TLR4 in recognition of gram-negative and gram-positive bacterial cell wall components. Immunity. 1999; 11:443–451. [PubMed: 10549626]

38. Bafica A, Scanga CA, Feng CG, Leifer C, Cheever A, Sher A. TLR9 regulates Th1 responses and cooperates with TLR2 in mediating optimal resistance to Mycobacterium tuberculosis. J Exp Med. 2005; 202:1715–1724. [PubMed: 16365150]

39. Liu PT, Stenger S, Li H, Wenzel L, Tan BH, Krutzik SR, Ochoa MT, Schauber J, Wu K, Meinken C, Kamen DL, Wagner M, Bals R, Steinmeyer A, Zugel U, Gallo RL, Eisenberg D, Hewison M, Hollis BW, Adams JS, Bloom BR, Modlin RL. Toll-like receptor triggering of a vitamin D-mediated human antimicrobial response. Science. 2006; 311:1770–1773. [PubMed: 16497887]

40. Shin DM, Yuk JM, Lee HM, Lee SH, Son JW, Harding CV, Kim JM, Modlin RL, Jo EK. Mycobacterial lipoprotein activates autophagy via TLR2/1/CD14 and a functional vitamin D receptor signalling. Cell Microbiol. 2010; 12:1648–1665. [PubMed: 20560977]

41. Yang CS, Shin DM, Kim KH, Lee ZW, Lee CH, Park SG, Bae YS, Jo EK. NADPH oxidase 2 interaction with TLR2 is required for efficient innate immune responses to mycobacteria via cathelicidin expression. J Immunol. 2009; 182:3696–3705. [PubMed: 19265148]

42. Cambier CJ, Takaki KK, Larson RP, Hernandez RE, Tobin DM, Urdahl KB, Cosma CL, Ramakrishnan L. Mycobacteria manipulate macrophage recruitment through coordinated use of membrane lipids. Nature. 2014; 505:218–222. [PubMed: 24336213]

43. Prados-Rosales R, Baena A, Martinez LR, Luque-Garcia J, Kalscheuer R, Veeraraghavan U, Camara C, Nosanchuk JD, Besra GS, Chen B, Jimenez J, Glatman-Freedman A, Jacobs WR Jr, Porcelli SA, Casadevall A. Mycobacteria release active membrane vesicles that modulate immune responses in a TLR2-dependent manner in mice. J Clin Invest. 2011; 121:1471–1483. [PubMed: 21364279]

44. Athman JJ, Wang Y, McDonald DJ, Boom WH, Harding CV, Wearsch PA. Bacterial Membrane Vesicles Mediate the Release of Mycobacterium tuberculosis Lipoglycans and Lipoproteins from Infected Macrophages. J Immunol. 2015; 195:1044–1053. [PubMed: 26109643]

45. Feltcher ME, Gibbons HS, Ligon LS, Braunstein M. Protein export by the mycobacterial SecA2 system is determined by the preprotein mature domain. J Bacteriol. 2013; 195:672–681. [PubMed: 23204463]

46. Schreiber HA, Harding JS, Hunt O, Altamirano CJ, Hulseberg PD, Stewart D, Fabry Z, Sandor M. Inflammatory dendritic cells migrate in and out of transplanted chronic mycobacterial granulomas in mice. J Clin Invest. 2011; 121:3902–3913. [PubMed: 21911937]

47. Davis JM, Ramakrishnan L. The role of the granuloma in expansion and dissemination of early tuberculous infection. Cell. 2009; 136:37–49. [PubMed: 19135887]

48. Nouailles G, Dorhoi A, Koch M, Zerrahn J, Weiner J 3rd, Fae KC, Arrey F, Kuhlmann S, Bandermann S, Loewe D, Mollenkopf HJ, Vogelzang A, Meyer-Schwesinger C, Mittrucker HW, McEwen G, Kaufmann SH. CXCL5-secreting pulmonary epithelial cells drive destructive neutrophilic inflammation in tuberculosis. J Clin Invest. 2014; 124:1268–1282. [PubMed: 24509076]

49. Caws M, Thwaites G, Dunstan S, Hawn TR, Lan NT, Thuong NT, Stepniewska K, Huyen MN, Bang ND, Loc TH, Gagneux S, van Soolingen D, Kremer K, van der Sande M, Small P, Anh PT, Chinh NT, Quy HT, Duyen NT, Tho DQ, Hieu NT, Torok E, Hien TT, Dung NH, Nhu NT, Duy PM, van Vinh Chau N, Farrar J. The influence of host and bacterial genotype on the development of disseminated disease with Mycobacterium tuberculosis. PLoS Pathog. 2008; 4:e1000034. [PubMed: 18369480]

50. Rath P, Huang C, Wang T, Wang T, Li H, Prados-Rosales R, Elemento O, Casadevall A, Nathan CF. Genetic regulation of vesiculogenesis and immunomodulation in Mycobacterium tuberculosis. Proc Natl Acad Sci U S A. 2013; 110:E4790–4797. [PubMed: 24248369]

51. Mayer-Barber KD, Andrade BB, Barber DL, Hieny S, Feng CG, Caspar P, Oland S, Gordon S, Sher A. Innate and adaptive interferons suppress IL-1alpha and IL-1beta production by distinct pulmonary myeloid subsets during Mycobacterium tuberculosis infection. Immunity. 2011; 35:1023–1034. [PubMed: 22195750]

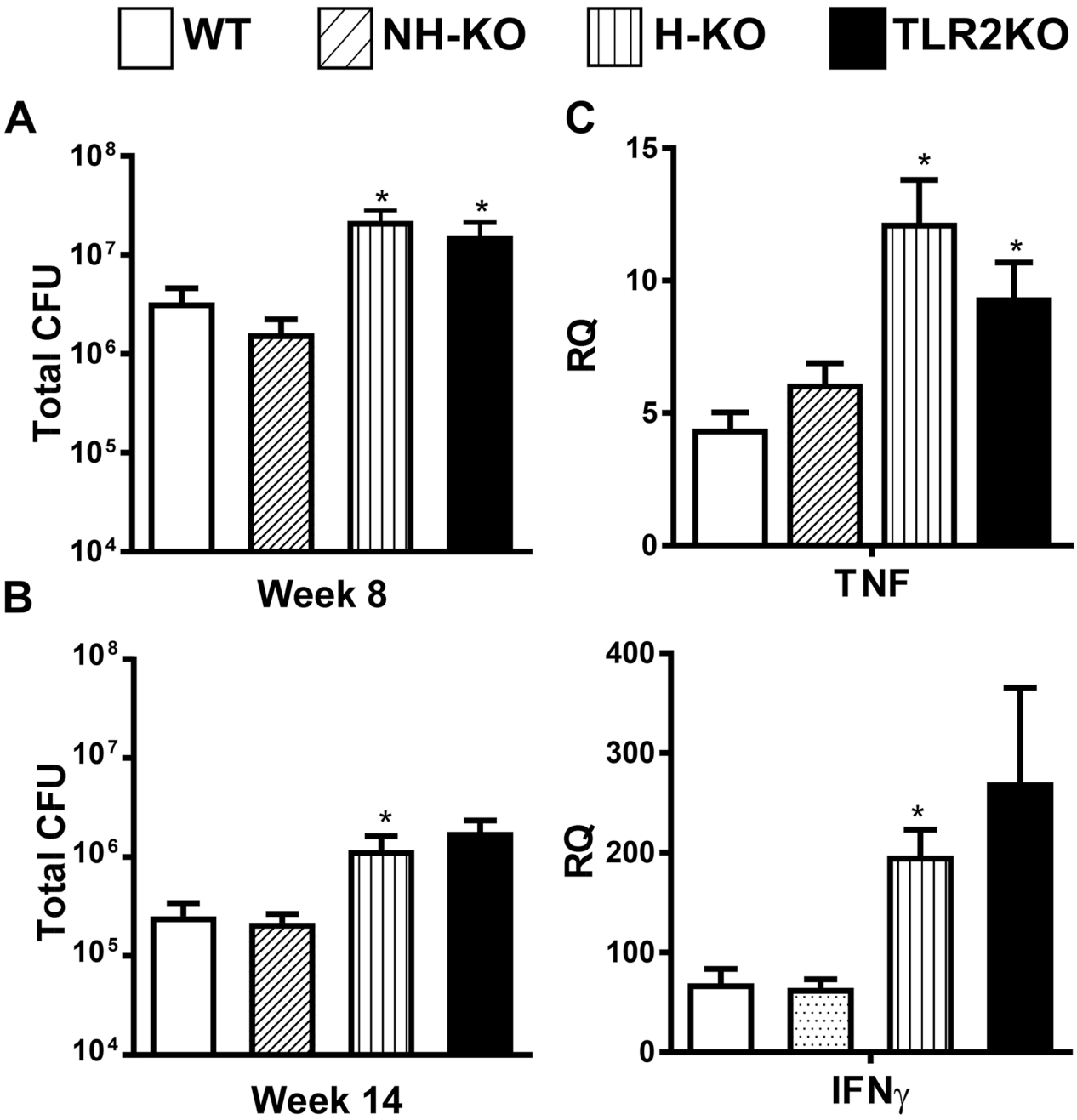

Figure 1. TLR2 signaling on hematopoietic cells contributes to control of bacterial burden during chronic Mtb infection

Pulmonary bacterial burden was evaluated in the lungs of bone marrow chimeric mice at 8 (A) and 14 (B) weeks following Mtb infection. NH-TLR2KO, H-TLR2KO, and TLR2KO chimeric mice were compared to WT mice. Time points were performed after separate aerosol infections with 4–5 mice used per group. The number of viable bacteria was determined by plating serial dilutions of lung homogenates onto 7H11 agar plates. Colonies were counted 21 days after incubation at 37°C to determine CFU in the lungs. Data are presented as mean CFU counts ± SEM. Significance was determined by Bonferroni Multiple

Comparisons test of One-Way ANOVA. *p<.05; **p<.01 *Denotes significance as compared to WT. Data is representative of two independent experiments with similar results. Expression levels of *Ifnγ* and *Tnf* in the lungs of 8 week infected mice (C) were determined by isolation of total lung RNA followed by RT-PCR analysis. PCR data includes 5 mice per group. All data is represented as mean ± SEM. Data is representative of two independent experiments. Significance was determined by unpaired T-test. *p< 0.05.

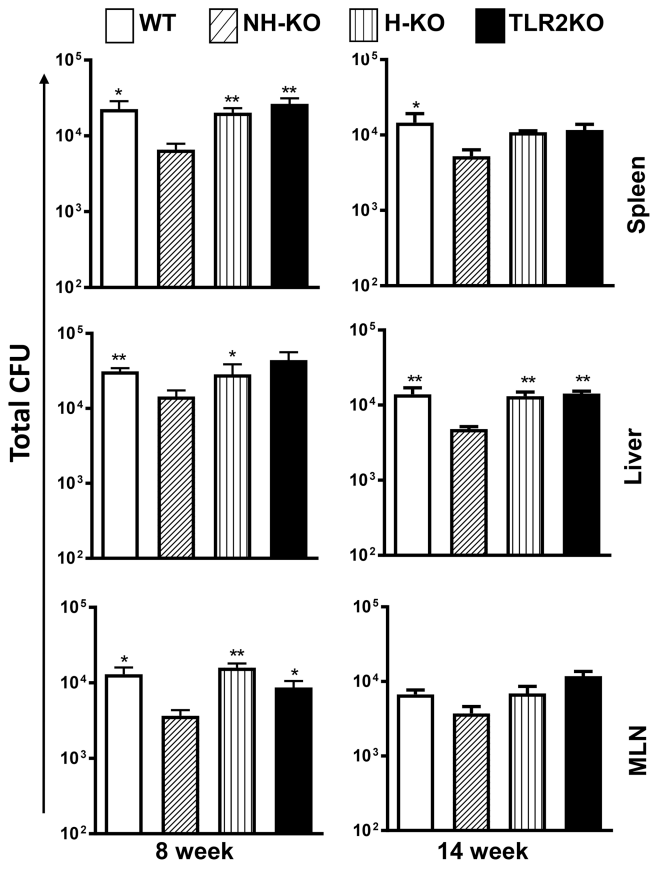

Figure 2. Dissemination of Mtb to extrapulmonary sites is influenced by TLR2 on non-hematopoietic cells

Bacterial burden in the spleen, liver, and mediastinal lymph nodes (MLN) was evaluated in bone marrow chimeric Mtb-infected mice at weeks 8 and 14. Time points were performed after separate aerosol infections with 4–5 mice used per group. The number of viable bacteria was determined by plating serial dilutions of homogenates onto 7H11 agar plates. Colonies were counted 21 days after incubation at 37°C to determine CFU. Data are presented as mean CFU counts ± SEM. Significance was determined by Bonferroni Multiple Comparisons test of One-Way ANOVA. *p<.05; **p<.01. *Denotes significance as compared to NH-TLR2KO. Data are representative of two independent experiments with similar results.

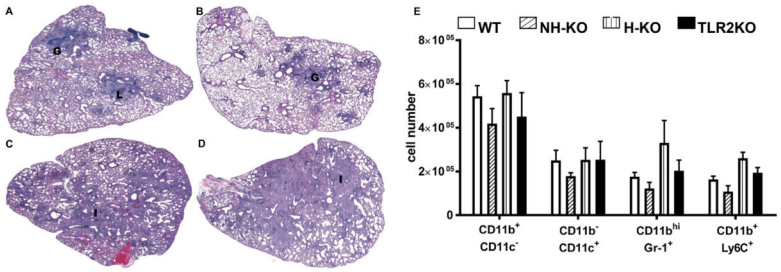

Figure 3. Absence of TLR2 on hematopoietic cells results in pneumonitis and loss of granuloma integrity

H&E stained sections of formalin-fixed paraffin-embedded tissues from the lungs of 8 week infected WT (A), NH-TLR2KO (B), TLR2KO (C), H-TLR2KO (D) chimeric mice. Images were created using Surveyor software with Turboscan by Objective Imaging at 20X. Figure is representative of 4–5 mice per group. Data is representative of 1 of 2 experiments. Lungs were harvested from WT, NH-KO, H-KO, and TLR2KO chimeric mice and single cell suspensions prepared and stained with a panel of antibodies reactive against CD11b, CD11c, GR1 and Ly6C to enumerate the following innate cell populations: $CD11b^{+}c^{-}$, $CD11b^{-}c^{+}$, $CD11b^{hi}Gr1^{+}$, $CD11b^{+}Ly6C^{+}$. Neutrophils and inflammatory monocytes were distinguished based on their SSC and expression level of CD11b. $SSC^{hI}CD11b^{hI}$ cells that expressed Gr-1 were labeled as neutrophils and $SSC^{lo}CD11b^{+}$ cells that expressed Ly6C were labeled as inflammatory monocytes (51). The data are presented as total cell numbers for each subset (E). Significance was determined by Bonferroni Multiple Comparisons test of One-Way ANOVA. Data are representative of two independent experiments with similar results. **p< 0.01.

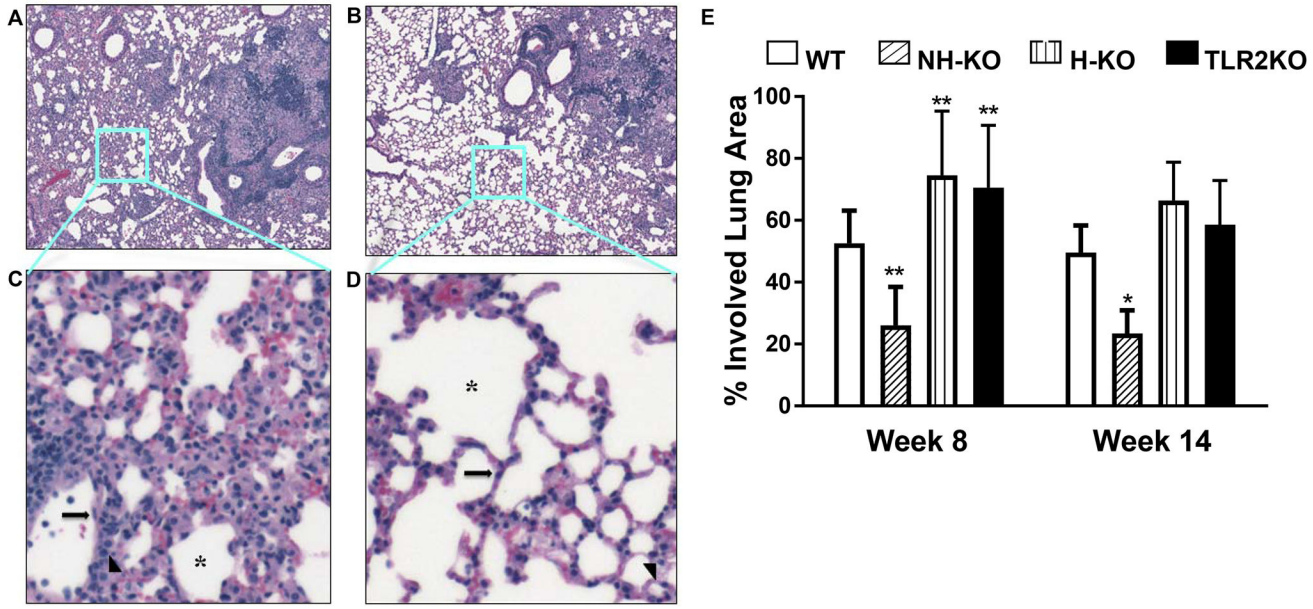

Figure 4. Granulomatous Inflammation is improved in the absence of TLR2 on non-hematopoietic cells

H&E stained sections of formalin-fixed paraffin-embedded tissues from the lungs of WT (A), NH-TLR2KO (B) chimeric mice obtained at 8 weeks post infection. Images were created using Surveyor software with Turboscan by Objective Imaging at 20X. Zoomed in sections (C and D) from mosaic images as designated by the light blue boxes in panels A and B. Long Arrow=type 1 pneumocyte; Arrowhead=type 2 pneumocyte; *denotes alveolar spaces. Percent of lung area involved in TB infection at week 8 and 14 determined using a grid layer in ImageProPlus (E). Data is shown as mean percentage ± SEM. Significance was determined by Bonferroni Multiple Comparisons Test for One-Way ANOVA as compared to WT. *$p<0.05$; **$p<0.01$. Data are representative of two independent experiments with similar results. Figure is representative of 4–5 mice per group.

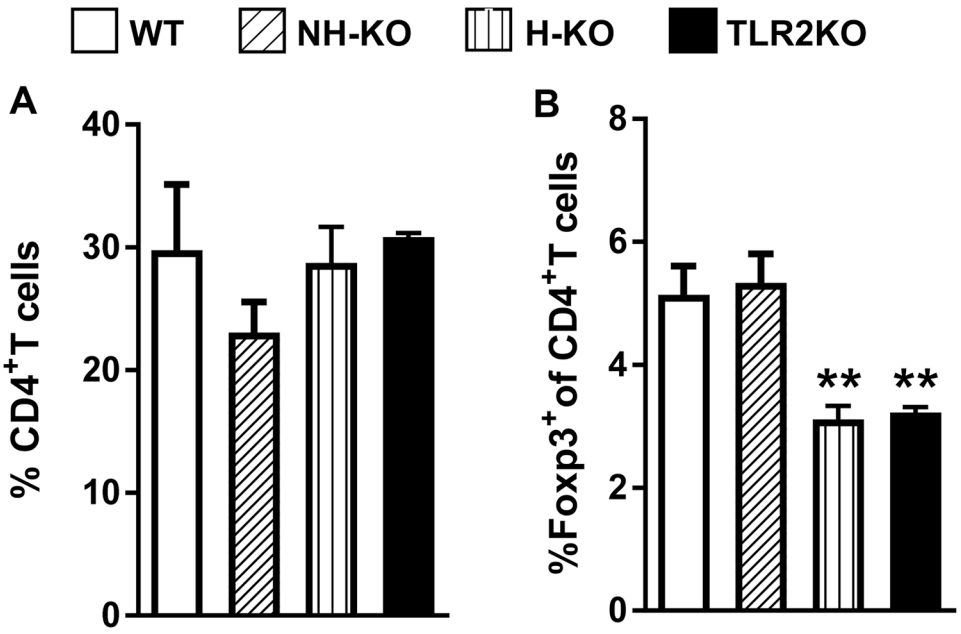

Figure 5.

Lungs were harvested from WT, NH-TLR2KO, H-TLR2KO, and TLR2KO chimeric mice and single cell suspensions prepared. Flow cytometry analysis was performed and the percentage $CD4^+$ T cells out of either $CD45.1^+$ or $CD45.2^+$ cells, as determined by the chimeric phenotype is presented (A). The percentage of $Foxp3^+$ cells is presented as a percentage out of gated $CD4^+$ cells (B). Data are presented as mean ± SEM. Significance was determined by Bonferroni Multiple Comparisons test of One-Way ANOVA. Data is representative of two independent experiments with similar results. **$p < 0.01$. Figure is representative of 4–5 mice per group.